Journal of Thermal Analysis and Calorimetry, Vol. 59 (2000) 289–303

Dedicated to Prof. Edith A. Turi in recognition of her leadership in education

MEASURING THE GLASS TRANSITION OF THERMOSETS BY ALTERNATING DIFFERENTIAL SCANNING CALORIMETRY

S. Montserrat

Departament de Màquines i Motors Tèrmics, Universitat Politècnica de Catalunya, Carrer de Colom 11, E-08222 Terrassa, Spain

Abstract

The glass transition temperature of thermosets is determined by alternating differential scanning calorimetry (ADSC), which is a temperature modulated DSC technique. The different values of the glass transition obtained from heat flow measurements (total and reversible) and heat capacity (modulus of the complex heat capacity) are analysed and compared with the values obtained by conventional DSC. The effect of the sample mass on the values of T_g, heat capacity and phase angle has been analysed. The effect of the thermal contact between sample and pan has been studied using samples cured directly inside the pan and disc-shaped samples of different thickness. The results obtained for the thermal properties and the phase angle are compared and analysed. The modulus of the complex heat capacity enables the determination of the dynamic glass transition, $T_{g\alpha}$, which is frequency dependent. The apparent activation energy of the relaxation process associated with the glass transition has been evaluated from the dependence of $T_{g\alpha}$ on the period of the modulation.

Keywords: epoxy resins, glass transition, thermosets, TMDSC

Introduction

The study of the glass transition of polymers is of great importance in the characterization of their thermal properties. One of the most widely used techniques to determine the glass transition is differential scanning calorimetry (DSC), but as a consequence of the kinetic nature of this transition, some precautions must be taken in its analysis. Thus, the value of the glass transition temperature depends on the thermal history of the sample. These problems and how to prevent them have been widely discussed in many books on fundamental calorimetry and thermal analysis [1–3].

More recently, temperature modulated differential scanning calorimetry (TMDSC) has received considerable attention since its introduction in 1993 [4–6]. This technique is based on the addition of a periodically varying temperature modulation to the linear heating (or cooling) rate, which has been applied extensively in the study of the glass transition [7]. One of the benefits of TMDSC is that it provides additional information on the glass transition, such as the determination of the dynamic glass transition, which depends on the frequency of the modulation. However, as the

1418–2874/99/ $ 5.00

Akadémiai Kiadó, Budapest
Kluwer Academic Publishers, Dordrecht

technique measures a heat flow which varies periodically, special care must be taken with respect to conventional DSC.

The aim of the present work is to measure the glass transition temperature (T_g) of thermosets by alternating differential scanning calorimetry (ADSC), which is a temperature modulated DSC technique, and also to show the effect of the sample size, by using samples of different mass, and the thermal contact between the sample and the pan, by using disc-shaped and pan-cured samples. The dynamic glass transition $T_{g\alpha}$, determined from the modulus of the complex heat capacity $|C_p^*|$ was determined in both samples and the effect of the frequency on $T_{g\alpha}$ is also analysed.

Alternating differential scanning calorimetry (ADSC)

ADSC is based on temperature modulation during a constant heating (cooling) rate, an idea that was initially proposed by Reading *et al.* [4–6]. In the non-isothermal experiments, the temperature T is programmed as a sinusoidal modulation of amplitude A_T and frequency ω (radian s^{-1}):

$$T = T_0 + q_0 t + A_T \sin(\omega t) \quad (1)$$

where T_0 is the initial temperature and q_0 is the underlying heating rate. The dependence of the heating rate on time is:

$$q = q_0 + A_T \omega \cos(\omega t) \quad (2)$$

From Eq. (2) it follows that the heating rate is obtained from the experimental parameters q_0, A_T and ω. The maximum and minimum values of q are obtained at the conditions of $q_{max}=q_0+A_T\omega$ and $q_{min}=q_0-A_T\omega$, respectively. An increase of the frequency and the temperature amplitude gives higher absolute values of q. At the same time, the absolute value of q increases with the underlying heating rate. The choice of these parameters is an important feature in order to obtain optimum conditions in TMDSC.

As a consequence of the periodical variation of q, a periodic heat flow signal is obtained which is shifted by a phase angle δ with respect to the heating rate. The Fourier transform of the cycles of the heating rate and the heat flow gives the following quantities:

q_0	underlying heating rate
$<HF>$	average or total heat flow
A_T	amplitude of the temperature modulation
A_{HF}	amplitude of the heat flow modulation
δ	phase angle between heat flow and heating rate

The average value of heat flow, also called total heat flow, is very similar to the signal obtained by conventional DSC at the same heating rate. The ratio of this quantity and q_0 defines an average or underlying heat capacity which practically corresponds to that obtained by conventional DSC [5, 8, 9]:

$$<C_p>=\frac{<HF>}{q_0} \tag{3}$$

Adopting the approach suggested by Schawe, based on linear response theory [10], a complex heat capacity may be defined

$$C_p^*=C_p'-iC_p'' \tag{4}$$

where C_p' is the in-phase heat capacity, and C_p'' the out-of-phase heat capacity. The modulus of C_p^* is:

$$\left|C_p^*\right|=\frac{A_{HF}}{A_q} \tag{5}$$

where A_q is the amplitude of the heating rate modulation ($A_q=A_T\omega$). The in-phase and out-of-phase heat capacities are defined as follows:

$$C_p' = |C_p^*| \cos\delta \tag{6}$$

$$C_p'' = |C_p^*| \sin\delta \tag{7}$$

Alternatively, the approach of reversing and non-reversing heat flow [4–6] defines the reversing heat flow, HF_{rev}, as $|C_p^*|q_0$, which one must multiply by –1 if heat flow is recorded with the endothermic direction downwards [11]. The non-reversing heat flow is defined as the difference between the total heat flow and the reversing heat flow.

These two methods of evaluating TMDSC data have been compared by Schawe [12] and the reversing component of the heat capacity has been identified with the modulus of the complex heat capacity, $|C_p^*|$. In the case of the glass transition, the phase angle is very small, thus according to Eq. (6) the values of $|C_p^*|$ and C_p' are indistinguishable. Similarly to the definition of non-reversing heat flow, the difference between the underlying heat capacity and the reversing component (equivalent to $|C_p^*|$, or C_p' in the glass transition) gives a non-reversing component of the heat capacity. This non-reversing component is not the same as the out-of-phase component of the heat capacity C_p'' [9, 12].

Experimental

An epoxy-amine resin and an epoxy-anhydride resin were used. The epoxy-amine was obtained from a commercial epoxy based on diglycidyl ether of bisphenol A (Araldite F from CIBA Speciality Chemicals), with an epoxy equivalent of 188.3 g equiv.$^{-1}$, cured by a triamine of polyoxypropylene (Jeffamine T-430 from Huntsman Corporation) at the stoichiometric ratio. The fully cured epoxy-amine (named FJ403) was obtained by curing for 3 h at 60°C together with a post-cure of 2 h at 180°C. The epoxy-anhydride was a commercial epoxy based on diglycidyl ether of bisphenol A (Araldite CY225 from CIBA Speciality Chemicals), with an epoxy equivalent of 200 g equiv.$^{-1}$, cured by a carboxylic anhydride derived from methyltetrahydrophthalic anhydride with accelerator (HY 225 from CIBA Speciality Chemicals) at the stoichiometric ratio. The fully cured epoxy (named CY225) was obtained by curing at 130°C for 12 h and at 160°C for 2 h.

The TMDSC measurements were performed by a Mettler Toledo 821e with an intracooler, and the ADSC evaluation of Mettler Toledo STAR© software was used. The temperature and heat flow calibrations and the determination of the time constant of the sensor were performed by standards of indium and zinc.

The usual modulation conditions used were an amplitude of 0.5 K and a period of 1 min, and an underlying heating rate (or cooling rate) of 1 K min^{-1}. In these conditions, the maximum and minimum heating rates are 4.14 and –2.14 K min^{-1}, respectively. In order to calibrate the heat flow signal, to correct the amplitude and eliminate the cell asymmetry a blank with an empty pan on the reference side and an empty pan plus a lid on the sample side was performed before the sample measurement. Conventional DSC measurements were performed using the same calorimeter at a heating rate of 10 K min^{-1}.

In both calorimetric experiments, DSC and ADSC, standard aluminium pans were used. The experiments were performed on samples cured directly inside the pan, where the mass was about 10 mg, and also on samples previously prepared as plates of different thickness and cut as discs of mass between 7 and 30 mg. The characteristics of these samples are indicated in Table 1.

Table 1 Nomenclature, sample form, mass and glass transition temperature by conventional DSC of the epoxy-amine (FJ403) and epoxy-anhydride (CY225) resins

Epoxy resin	Code	Sample form	Mass/mg	T_{g_m}/°C[c]
FJ403	P7	Cured inside pan[a]	10.58	84.6
FJ403	P10	Cured inside pan[a]	10.05	83.5
FJ403	P16	Cured inside pan[a]	9.85	83.9
FJ403	P22	Cured inside pan[a]	9.97	84.8
FJ403	A	disc[b]	7.88	83.3
FJ403	B	disc[b]	16.3	86.9
FJ403	C	disc[b]	30.41	86.8
CY225	CY225	disc[b]	12.15	107.9

[a]Sample cured directly inside the aluminium pan
[b]Sample cured as a plate and cut in discs
[c]Midpoint glass transition by conventional DSC at a heating rate of 10 K min^{-1}

In order to ensure the same thermal history in the determination of the glass transition, the sample was heated 20°C above T_g for 5 min and then quenched to a temperature well below T_g (about T_g–60°C). The sample was then immediately reheated at the indicated heating rate and T_g was measured during this scan. The determination of T_g by cooling was performed at the indicated cooling rate from a temperature of about 40°C above T_g to a temperature well below T_g. As is usual in calorimetry, T_g is assigned to the temperature at which the specific heat capacity is midpoint between its glassy and liquid values during a heating (or cooling) scan at the indicated experimental conditions. This temperature is usually called midpoint glass transition, T_{gm}.

Results and discussion

Glass transition of the fully cured epoxy from ADSC signals

The glass transition temperature has been evaluated by ADSC from both the heat flow signal and heat capacity measurements. As pointed out above, the T_g determined from the total heat flow signal is practically equal to the value obtained by conventional DSC at the same heating rate. Figure 1 shows the total heat flow signal obtained in the epoxy resin cured inside the pan by ADSC at 1 K min^{-1}. As was expected, the midpoint glass transition temperature from the total heat flow, at 1 K min^{-1}, is lower than that obtained by DSC at 10 K min^{-1}, as shown in Table 2. Figure 1 also includes the reversing heat flow signal HF_{rev}, the modulus of the complex heat capacity $|C_p^*|$ and the in-phase heat capacity C_p'.

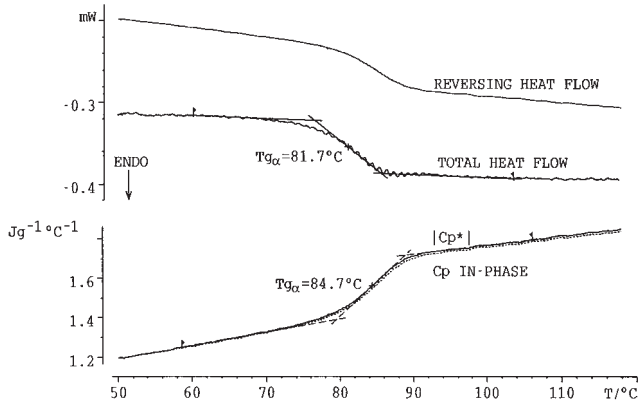

Fig. 1 Heat flow and heat capacity curves of the fully cured epoxy resin FJ403 (sample P22) in the glass transition region, obtained at an underlying heating rate of 1 K min^{-1}, 0.5 K of amplitude and 1 min of period: total heat flow and reversing heat flow, modulus of the complex heat capacity and in-phase heat capacity. The values of the glass transition temperature determined in the total heat flow and $|C_p^*|$ curves are indicated

However, the heat flow signal from ADSC shows ripples superimposed on the underlying signal, which introduces an inaccuracy into the measurement of the midpoint T_g. The frequency and size of these ripples depends on the modulation conditions, and their origin is a consequence of the Fourier transform of the modulated heat flow signal in the ADSC procedure [13, 14]. They are also always present in the other ADSC signals, such as the reversing heat flow, the complex heat capacity values and the phase angle in the glass transition measurements, unless a data smoothing routine is used. A theoretical analysis of the glass transition by TMDSC using a single-parameter theoretical model shows these ripples in the total C_p, C_p', C_p'' and δ (Fig. 1 of [9]). Similarly, Wunderlich and Okazaki [15], using a model based on the

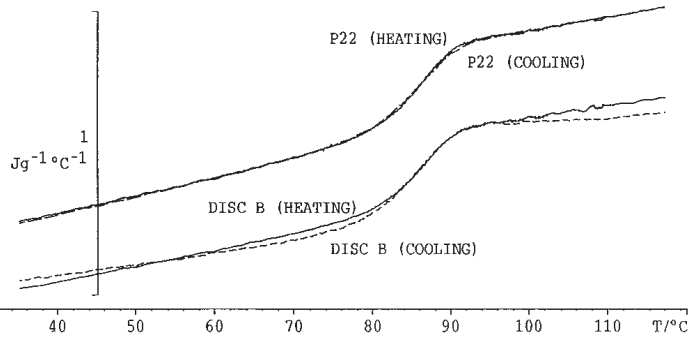

Fig. 2 Modulus of the complex heat capacity for the epoxy resin FJ403 cured inside the pan (sample P22) and in discs (sample disc B) obtained by heating (solid line) and cooling (dashed line). The heat capacity scale is relative. The modulation conditions were q_0=1 K min^{-1}, A_T=0.5 K and t_p=1 min

hole theory, show periodic changes in the total C_p and first harmonic component ('reversing' heat capacity) curves (Fig. 3 of [15]).

Table 2 Average values of the glass transition temperature of the fully cured epoxy FJ403 cured inside the pan determined by DSC and ADSC

	q_0/K min^{-1}	T_{go}[(a)]/°C	T_{gm}[(b)]/°C	T_{ge}[(c)]/°C	Averaged scans[(d)]
DSC	10	79.2±0.8	84.2±0.6	89.3±0.4	4[(e)]
ADSC, $\|C_p^*\|$	1	79.8±0.5	84.7±0.7	89.4±0.9	5[(f)]
ADSC, $\|C_p^*\|$	–1	90.4±0.6	84.2±0.8	78±1	2[(f)]
ADSC, HF rever.	1	79.9±0.5	84.9±0.5	90.2±0.7	5[(f)]
ADSC, HF total	1	77.6±0.8	82.4±0.8	86.5±0.8	5[(f)]

ADSC: modulation of 0.5 K and 1 min
[(a)] T_{go} – onset glass transition temperature
[(b)] T_{gm} – glass transition temperature at the midpoint between the glassy and liquid values
[(c)] T_{ge} – endset glass transition temperature
[(d)] Number of scans averaged to obtain the indicated value of T_g
[(e)] Scans of samples P5, P10, P16 and P22
[(f)] Scans of samples P10 and P22

The glass transition temperature may be determined by complex heat capacity measurements. The modulus of the heat capacity $|C_p^*|$ shows a sigmoidal signal in the glass transition region. The dynamic glass transition is defined by the temperature at the midpoint heat capacity change, $T_{g\alpha}$ (Fig. 1). This variation in $|C_p^*|$ may be justified in terms of the relaxation time of the chain segments $<\tau>$ [9, 16, 17]. At a temperature below the glass transition region, $<\tau>$ is much longer than the cycle period, t_p, and the amplitude of the oscillating part reflects a glassy response giving a $|C_p^*|_g$ value. At a temperature above

the glass transition, $<\tau>$ is shorter than t_p and the system shows a $|C_p^*|_l$ of the liquid state which is higher than $|C_p^*|_g$. In the transition interval, the heat capacity increases from $|C_p^*|_g$ to $|C_p^*|_l$ and there is a temperature where $<\tau>=t_p$. This is the dynamic glass transition temperature $T_{g\alpha}$, which may be estimated at the midpoint of the change of $|C_p^*|$. This $T_{g\alpha}$ depends on the frequency of the modulation ω. An increase of ω corresponds to a decrease in t_p and gives a higher $T_{g\alpha}$. This dependence will be analysed below.

As the modulus of the complex heat capacity $|C_p^*|$ is used to evaluate the HF_{rev} multiplied by the underlying heating rate, it follows that the value of $T_{g\alpha}$ is equal to that obtained from HF_{rev}, which is confirmed by the values shown in Table 2 ($T_{g\alpha}$ is 84.2±0.8 and T_{gm} from HF_{rev} is 84.9±0.5).

In the samples cured inside the pan, the experiments performed by cooling give values of $T_{g\alpha}$ which are practically equal to those obtained by heating at the same rate, as shown in Table 2. Moreover, the shape of the $|C_p^*|$ curve obtained by heating is practically identical to the $|C_p^*|$ curve obtained by cooling (sample P22 in Fig. 2). In contrast, in the case of the disc-shaped samples, a slight difference is observed in the shape of $|C_p^*|$ during heating and cooling scans (sample disc B in Fig. 2).

In the glass transition measurements, the phase angle is very small and therefore, according to the definition of the in-phase heat capacity, C_p', given by Eq. (6), the modulus of the complex heat capacity is practically equal to C_p'. This behaviour may be clearly observed in the epoxy sample cured inside the pans shown in Fig. 1, where the phase angle is between –0.05 and –0.14 radians, and cosδ≈1, resulting in a coincidence of $|C_p^*|$ and C_p' curves. Figure 3 shows the values of the uncorrected phase angle of this sample. On the other hand, C_p'' shows a peak in the glass transition region (Fig. 3), the area of which may be related to the entropy generation due to the irreversibility of the process [18].

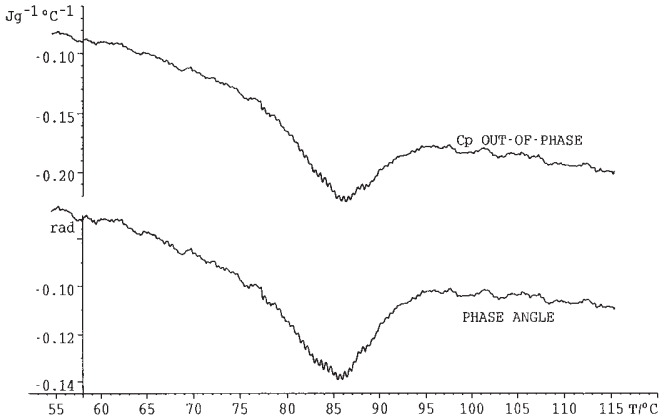

Fig. 3 Curves of the uncorrected out-of-phase heat capacity and uncorrected phase angle for the epoxy FJ403 cured inside the pan (sample P22). The modulation conditions are the same as in the above figures: q_0=1 K min^{-1}, A_T=0.5 K and t_p=1 min

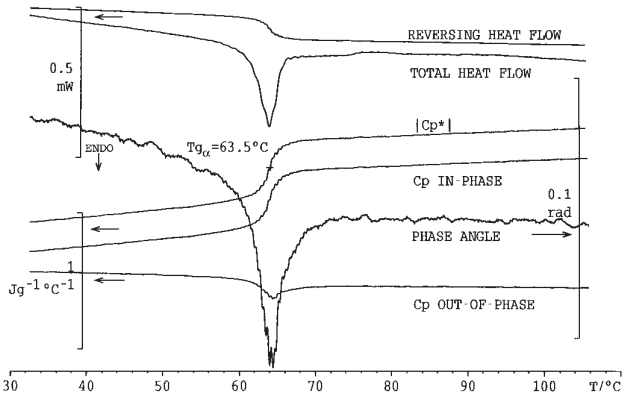

Fig. 4 Heat flow (total and reversing), heat capacity ($|C_p^*|$, C_p' and C_p'') and phase angle curves of an epoxy resin FJ403 partially cured inside the pan (cured 24 h at 50°C) obtained at 1 K min^{-1}, 0.5 K of amplitude and 1 min of period. The heat flow, heat capacity and phase angle scales are relative

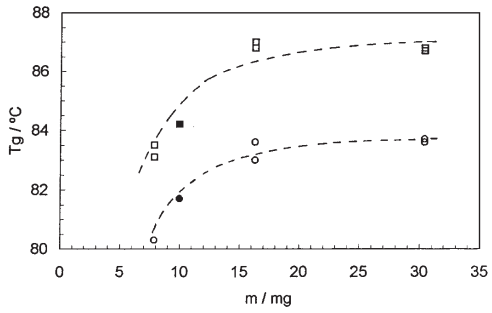

Fig. 5 Dependence of the midpoint glass transition temperature obtained from the heat flow on the sample mass using samples of different thickness (samples A, B and C): values obtained by conventional DSC at 10 K min^{-1} (□) and from the total heat flow signal obtained by ADSC at 1 K min^{-1} (○). The filled symbols correspond to a sample cured directly inside the pan (sample P22). The modulation conditions were 0.5 K and 60 s. The lines are a guide for the eye

In samples submitted to physical ageing, the total heat flow signal shows the typical endothermic peak, while the reversing heat flow does not show any relaxational effect. This effect is shown in Fig. 4 in the epoxy FJ403 partially cured at 50°C for 24 h, resulting in a conversion of 85%. The glass transition temperature of this epoxy is 63.5°C and has been aged at 50°C after vitrification of the system, which takes place at 7.9 h [19]. The variation of $|C_p^*|$ is also sigmoidal, as in non-aged samples, but a more abrupt change of $|C_p^*|$ in the glass transition is seen. The interval of the glass transition measured by the difference between the extrapolated endset and onset temperatures is about 2°C in the partially cured epoxy, whereas it is about 10°C in the fully cured epoxy. This effect has also been observed in the physical ageing of the fully cured epoxy CY225 [20].

Effect of mass and thermal contact between sample and pan on the glass transition

All the values of the glass transition temperature shown in the preceding section were referred to epoxy samples of practically the same mass and cured inside the pan, which ensures a very good thermal contact between the sample and the bottom of the pan. Let us now describe the effect observed on the glass transition when disc-shaped samples of different mass were used.

A dependence of the glass transition temperature, T_{gm}, obtained by DSC at 10 K min^{-1} on mass is observed in Fig. 5. The T_{gm} increases from about 83 to 87°C when the mass changes from 8 to 30 mg. In a set of melting experiments using indium samples of masses between 6 and 38 mg, the onset temperature was practically constant, showing values of about 156.5°C. Taking into account the different thermal conductivity of the epoxy and indium samples, the dependence observed in the epoxy resin is attributed to the low thermal conduction coefficient.

The results of T_{gm} obtained by ADSC from the total heat flow also show a similar dependence on the mass, but these values are lower than those obtained by conventional DSC as a consequence of the lower heating rate (Fig. 5). The dynamic glass transition temperature $T_{g\alpha}$, obtained from the midpoint in the $|C_p^*|$ signal, also shows an increase with mass tending to constancy for masses higher than 16 mg (Fig. 6).

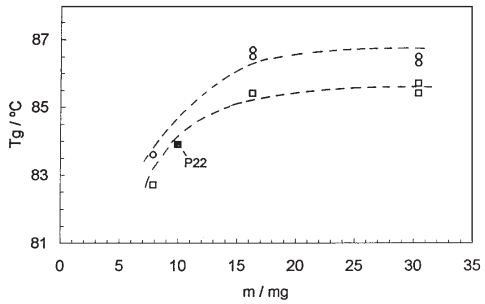

Fig. 6 Dependence of midpoint glass transition temperature obtained from heat capacity measurements on the sample mass using samples of different thickness (samples A, B and C). Values obtained by ADSC at 1 K min^{-1} for $|C_p^*|$ (□) and C_p' (○). The filled symbols correspond to sample P22 (epoxy cured directly inside the pan) where $|C_p^*|$ is practically equal to C_p'. The modulation conditions were 0.5 K and 60 s. The lines are a guide for the eye

In disc-shaped samples of different thickness, the T_g determined from the midpoint in the in-phase heat capacity C_p' is slightly higher than the T_g determined from $|C_p^*|$. This difference is between 1 and 1.5°C (Fig. 6). As shown below, this difference is a consequence of the higher phase angle δ which means that cosδ <1, and C_p' becomes different from $|C_p^*|$. In contrast, in samples cured inside the pan, the phase angle is very small and T_g determined by C_p' is practically equal to T_g obtained by $|C_p^*|$ as shown in Fig. 6.

Table 3 Values of $|C_p^*|$ in J (g K)$^{-1}$ at 50 and 110°C for heating and cooling scans for different samples of the epoxy FJ403

Sample	Heating scans		Cooling scans	
	$\|C_p^*\|_g$ at 50°C	$\|C_p^*\|_l$ at 110°C	$\|C_p^*\|_g$ at 50°C	$\|C_p^*\|_l$ at 110°C
A	0.93	1.48	1.25	1.78
B	0.91	1.46	1.23	1.73
C	0.96	1.47	1.30	1.77
P10	1.15	1.81	1.16	1.80

The curves of $|C_p^*|$ obtained by cooling show practically the same value of $T_{g\alpha}$ as in the heating scan (differences not higher than 0.5°C have been observed), but the shape is different when disc-shaped samples are used, as shown in Fig. 2. Table 3 shows the differences observed in $|C_p^*|_g$ and $|C_p^*|_l$ in these samples. In the zone of the glassy state, at 50°C, the values of $|C_p^*|_g$ in the heating scan are about 0.3 J (g K)$^{-1}$ lower than in the cooling scan, as shown in Table 3. A similar difference is observed in the zone of the liquid state at 110°C. These differences were observed for all the disc-shaped samples, but are practically negligible for samples cured inside the pan. Table 3 also shows that the values of $|C_p^*|$ in the glassy (or in the liquid state) for disc-shaped samples are practically constant in the mass interval analysed in this work (7 to 30 mg). However, Wunderlich *et al.* have found a strong dependence of $|C_p^*|$ on mass for samples of sapphire standard higher than 60 mg (Fig. 7 in [21]).

Phase angle in the glass transition region

The phase angle measures the shift of the modulated heat flow signal with respect to the heating rate. In an ideal system with an infinitely good heat transfer, δ must be zero if there are any thermal events. In the glass transition region there is a delay of the heat flow with respect to the heating rate and a variation of δ is observed as a consequence of the relaxation process. This variation has been simulated theoretically using a single parameter model (Fig. 1 in [9]), and a peak in the phase angle signal is observed in the glass transition region. This peak is frequency dependent as a consequence of the relaxational behaviour of the glass transition.

The TMDSC experiments performed on polymers show a non-zero value of the phase angle even in the glassy state or in the liquid state. This non-zero value of the phase angle is due to the strong dependence of the phase angle on the heat conductance of the sample, and to the thermal contact between the sample, the bottom of the pan and the thermometer of the calorimetric cell [22]. The phase angle also depends on the modulation frequency and the heat capacity, and may be expressed as:

$$\tan\delta_{ht} = \frac{\omega m C_p}{K} \tag{8}$$

and for small angles, as in the glass transition region (δ<0.5 rad), it follows that

$$\delta_{ht} \approx \frac{\omega m C_p}{K} \tag{9}$$

where K is the heat conductance of the heat flow from the sample to the thermometer. During the glass transition an additional phase angle δ_r is superimposed onto δ_{ht}. In order to obtain the phase angle corresponding to the relaxation a correction method has been introduced by Schick *et al.* [22]. This method has been adapted to ADSC measurements by Hutchinson *et al.* [23].

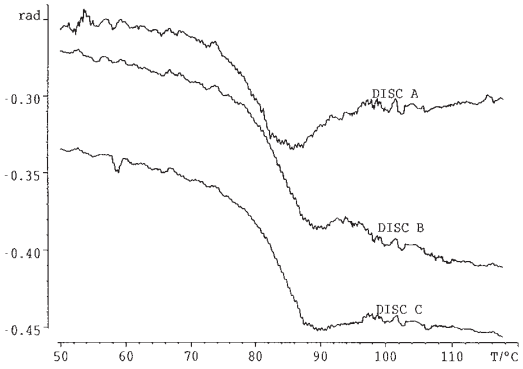

Fig. 7 Uncorrected phase angle for the epoxy FJ403 in disc-shaped samples (samples A, B and C). The modulation conditions were q_0=1 K min^{-1}, A_T=0.5 K and t_p=1 min

The uncorrected or experimental phase angle for the epoxy FJ403 cured inside the pan is shown in Fig. 3. The phase angle is negative and shows a peak in the region of the glass transition. In the glassy state, the heat capacity increases quasi-linearly with temperature (Fig. 1) and according to Eq. (9), the absolute phase angle $|\delta|_g$ shows a similar linear variation as far as the glass transition region. In this zone, the variation of the phase angle due to relaxation is added to the phase angle due to the heat transfer and $|\delta|$ shows the above-mentioned relaxation peak. In the liquid state, the phase angle $|\delta|_l$ increases with respect to $|\delta|_g$ due to the increase of the heat capacity in the liquid state. This different value confers an asymmetry to the peak.

The effect of mass and thermal contact on phase angle in disc-shaped samples (discs A, B and C) is shown in Fig. 7. The peak associated to the glass transition is broader than in the samples cured inside the pan, which may be attributed to a worse thermal contact between sample and pan. It is also observed an increase of the absolute phase angle with the sample mass (and sample thickness) due to the dependence of δ_{ht} on both the mass and the heat conductance inside the sample or between sample and pan. Similar behaviour (not shown in this paper) of the disc-shaped and pan-cured samples has been observed in the epoxy-anhydride system CY225.

In order to obtain a corrected phase angle, Schick's method [22] was applied. This method is based on the assumption that the baseline to correct the phase angle is the change of the C_p^* modulus, previously inverted and appropriately scaled. Figure 8

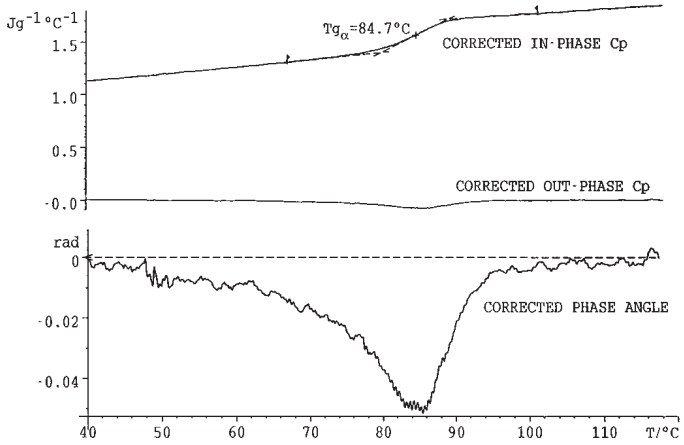

Fig. 8 Corrected curves of the in-phase and out-of-phase heat capacity and the corrected phase angle of the same sample shown in Figs 1 and 3. The correction was based on Schick's method [22]

shows the correction of the C'_p, C''_p and phase angle corresponding to the ADSC curves shown in Fig. 1 above. It is observed that the value of T_g obtained from the corrected C'_p in Fig. 8 is practically the same as that obtained from the uncorrected C'_p in Fig. 1 due to the low value of the phase angle.

Dependence of $T_{g\alpha}$ on the period of modulation

As mentioned above, the glass transition $T_{g\alpha}$ measured as the midpoint temperature of the variation of $|C^*_p|$ depends on the frequency of modulation. Figure 9 shows the shift of the curves of $|C^*_p|$ to higher temperatures when the period of modulation decreases. It is also observed a decrease of the variation of the complex heat capacity $\Delta|C^*_p|$ at the glass transition when the period decreases. This dependence may be attributed to heat transfer effects between sample and pan. A more extensive study about this dependence is currently in progress.

The dependence of $T_{g\alpha}$ on $\ln(t_p)$ may be derived from an empirical equation of the relaxation time τ as a function of the temperature and the structure of the glass (defined by the enthalpy excess ∂). One equation that is used in the single parameter model [24] is

$$\tau = \tau_o \exp[-\theta(T - T_g)] \exp[-(1 - x)\, \theta\partial/\Delta C_p] \qquad (10)$$

where x is the non-linearity parameter, which is a partitioning parameter ($0 \le x \le 1$) defining the relative contributions of the temperature and structure on the relaxation time, and θ is a parameter characterising the temperature dependence of τ in equilibrium conditions, which is related to an apparent activation energy of the relaxation process Δh^* by the relation $\theta \approx \Delta h^*/RT_g^2$. Assuming that the glass transition occurs approximately at the midpoint temperature of the variation of $|C^*_p|$ when $<\tau>=t_p$, and

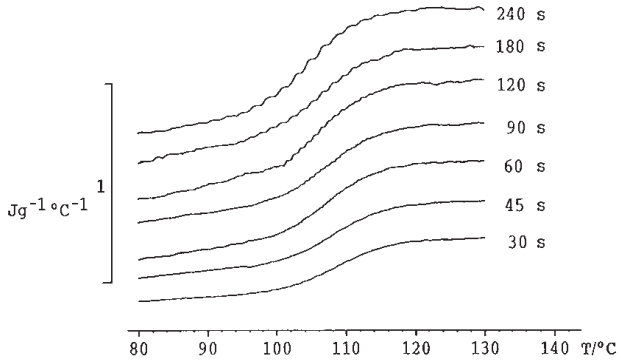

Fig. 9 Effect of period of modulation on the modulus of the complex heat capacity for the epoxy CY225. Experimental conditions: q_0=1 K min^{-1}, A_T=0.5 K and t_p between 30 and 240 s

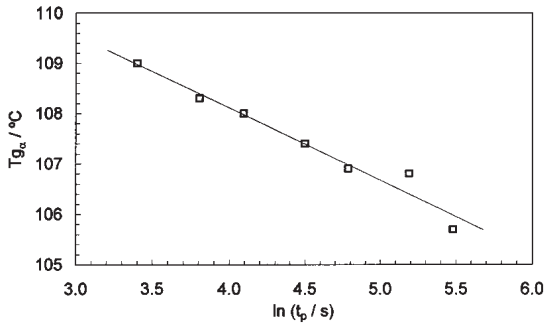

Fig. 10 Dependence of the dynamic glass transition on the period for the epoxy CY225. The line corresponds to a linear regression

that the effect of structure is ignored by neglecting the second exponential term in Eq. (10), it follows that

$$\frac{\mathrm{d}\ln t_p}{\mathrm{d}(T_{g\alpha})}=-\theta \tag{11}$$

Figure 10 shows the plot of $T_{g\alpha}$ *vs*. ln(t_p) for the epoxy-anhydride system CY225, giving a slope of $-1/\theta=-1.437$ K, with a regression coefficient r^2 of 0.96. Then, $\theta=0.696$ K^{-1}, and taking an average value of T_g=107°C, the activation energy $\Delta h^*/R$ is 100 kK. These experiments were performed at a heating rate of 1 K min^{-1}, an amplitude of 0.5 K and a period of between 30 s and 240 s.

At the same time, the $\Delta h^*/R$ may be calculated from intrinsic cycles by conventional DSC. These experiments are performed by cooling the sample at different cooling rates q_c (from 160 to 0.5 K min^{-1}) and immediately reheating at a heating rate which is always the same (10 K min^{-1}). The apparent activation energy Δh^* is calcu-

lated from the dependence of the fictive temperature, T_f, calculated in each experiment, on the cooling rate q_c [25]:

$$\frac{\Delta h^*}{R}=-\left[\frac{\partial \ln|q_c|}{\partial(1/T_f)}\right] \tag{12}$$

The value calculated by this method in the fully cured epoxy CY225 was 132 kK [26]. The different value obtained by ADSC may be attributed to experimental causes as the limitation in the range of frequencies from 33 mHz (t_p=30 s) to 4 mHz (t_p=240 s), approximately one decade of frequency values. In conventional DSC the range of cooling rates was about 4 decades [26]. On the other hand, Eq. (10) is based on an Arrhenius dependence of the relaxation times and other authors [27] have shown better fits to the Vogel-Fulcher-Tammann dependence when a wide interval of frequencies is used.

Conclusions

The glass transition temperature of an epoxy-amine resin has been evaluated by ADSC, which is a TMDSC technique. The total heat flow signal gives a glass transition temperature T_{gm} which is equivalent to that measured by conventional DSC at the same heating rate. At the same time, the modulus of the complex heat capacity allows the evaluation of the dynamic glass transition $T_{g\alpha}$, which is frequency dependent. The values of T_{gm} and $T_{g\alpha}$ show an increase with the sample mass, and tend to be constant for masses higher than 16 mg. A similar result has been observed in the measurements of the glass transition temperature by conventional DSC. This effect is not observed in the onset temperature of the melting of standard indium samples and may be attributed to the lower thermal conduction coefficient of the thermosets in comparison with the metallic sample.

The effect of the thermal contact between sample and pan has been analysed by comparing results obtained in epoxy samples cured inside the pan and disc-shaped samples of different thickness. In samples cured inside the pans the phase angle is very low, $\cos\delta\approx1$, and $C_p'\approx|C_p^*|$. Then, the correction of the angle phase is not necessary in order to obtain C_p' and C_p''. Likewise, $|C_p^*|$ shows a reversing behaviour because the curves obtained by heating and cooling are practically coincident. On the other hand, the disc-shaped samples show higher absolute values of the phase angle as a consequence of the increase of the sample mass and thickness, which affects the thermal conductance inside the sample or between sample and pan. As a result of this increment of the phase angle, C_p' is different from $|C_p^*|$; thus, it is necessary to correct the phase angle in order to measure C_p' and C_p''. In these samples, the reversibility of $|C_p^*|$ by heating and cooling is not observed. In addition, the increase of the sample mass also raises the absolute value of the phase angle, contributing to shift the C_p' with respect to $|C_p^*|$.

Finally, the dependence of $T_{g\alpha}$ on the period has been shown for an epoxy-anhydride resin. As the $T_{g\alpha}$ occurs when the relaxation time $<\tau>$ equal t_p, it follows that an increase of the period will shift $T_{g\alpha}$ to lower values. This dependence enables

the determination of an apparent activation energy which characterises the relaxation process associated with the glass transition.

* * *

Financial support has been provided by CICYT Project No. MAT 97-0634-C02-02. The author is grateful to CIBA Speciality Chemicals and Hunstman Corporation for supplying the materials.

References

1 E. A. Turi ed., Thermal Characterization of Polymeric Materials, Academic Press, San Diego 1997, Vol. 1, Chap. 3.
2 V. B. F. Mathot Ed, Calorimetry and Thermal Analysis of Polymers, Hanser Publ. Munich 1994, Chap. 6.
3 G. W. H. Höhne, W. Hemminger and H. J. Flammersheim, Differential Scanning Calorimetry. An Introduction for Practitioners, Springer, Berlin 1996, Chap. 6.
4 M. Reading, Trends Polym. Sci., 1 (1993) 248.
5 M. Reading, D. Elliot and V.L. Hill, Proceedings of 21st NATHAS (1992) 145; J. Thermal Anal., 40 (1993) 949.
6 S. Gill, S.R. Sauerbrunn and M. Reading, J. Thermal Anal., 40 (1993) 931.
7 Special Issue on Temperature Modulated Calorimetry, C. Schick and G. W. H. Höhne eds., Thermochim. Acta, 304/305 (1997)
8 A. Boller, C. Schick and B. Wunderlich, Thermochim. Acta, 266 (1995) 97.
9 J. M. Hutchinson and S. Montserrat, Thermochim. Acta, 304/305 (1997) 257.
10 J. E. K. Schawe, Thermochim. Acta, 261 (1995) 183.
11 B. Wunderlich, Y. Jin and A. Boller, Thermochim. Acta, 238 (1994) 277.
12 J. E. K. Schawe, Thermochim. Acta, 260 (1995) 1.
13 J. M. Hutchinson, Mettler Toledo USER COM no.6 (1997) 22.
14 J. M. Hutchinson, A. B. Tong and Z. Jiang, Thermochim. Acta, 335 (1999) 27.
15 B. Wunderlich and I. Okazaki, J. Thermal Anal., 49 (1997) 57.
16 J.M. Hutchinson and S. Montserrat, J. Thermal Anal., 47 (1996) 103.
17 J. M. Hutchinson and S. Montserrat, Thermochim. Acta, 286 (1996) 263.
18 J. E. K. Schawe, Thermochim. Acta, 304/305 (1997) 111.
19 S. Montserrat and I. Cima, Thermochim. Acta, 330 (1999) 189.
20 S. Montserrat, Proceedings of 4th Mediterranean Conference on Calorimetry and Thermal Analysis, Patras (Greece) 1999.
21 B. Wunderlich, J. Thermal Anal., 42 (1994) 307.
22 S. Weyer, A. Hensel and C. Schick, Thermochim. Acta, 304/305 (1997) 267.
23 Z. Jiang, C. T. Imrie and J. M. Hutchinson, Thermochim. Acta, 315 (1998) 1.
24 A. J. Kovacs, J. J. Aklonis, J. M. Hutchinson and A. R. Ramos, J. Polym. Sci., Polym. Phys. Ed., 17 (1979) 1097.
25 C. T. Moynihan, A. J. Easteal, M. A. DeBolt and J. Tucker, J. Am. Ceram. Soc., 59 (1976) 12.
26 S. Montserrat, P. Cortés, A. Pappin, K. H. Quah and J. M. Hutchinson, J. Non-Crystal. Solids, 172–174 (1994) 1017.
27 A. Hensel, J. Dobbertin, J. E. K. Schawe, A. Boller and C. Schick, J. Thermal Anal., 46 (1996) 935.